Electronic Supplementary Material (ESI) for Sustainable Energy & Fuels.

ETHANOL TO DIESEL: A SUSTAINABLE ALTERNATIVE FOR THE HEAVY-DUTY TRANSPORTATION SECTOR

Juan-Manuel Restrepo-Flórez[1,2*], Paolo Cuello-Peñaloza[1*], Emmanuel Canales[1], Dustin Witkowski[2], David A. Rothamer[2], George Hubber[1], and Christos T. Maravelias[3,4]

[1]Department of Chemical and Biological Engineering, University of Wisconsin–Madison

[2]Department of Mechanical Engineering, University of Wisconsin–Madison

[3]Department of Chemical and Biological Engineering, Princeton University

[4]Andlinger Center for Energy and the Environment, Princeton University

**These authors contributed equally to this paper*

Index

SI-1 Financial parameters

Table S1. Financial and cost assumptions used in this study.

General parameters		**Source**
Reference year		2021
Reference capacity	504 Ton/day	1
Financial variables		
Equity	40%	1
Loan interest	8%	
Loan term (years)	10	
Operation period (years)	30	
Depreciation period (years)	7	
Construction period (years)	3	
% year -2	8%	
% year -1	60%	
% year 0	32%	
Startup time (years)	0.25	
Feedstock use during start up (% of Normal)	50%	
Variable cost during start up (% of Normal)	75%	
Fixed cost during start up (% of Normal)	100%	
Discount rate	10%	
Income tax	21%	
Working capital (% of FCI)	5%	
Base year for analysis	2007	
Direct costs		
OSBL (% of ISBL)	40%	1
Warehouse (% of ISBL)	4%	
Site development (% of ISBL)	9%	
Additional piping (% of ISBL)	4.5%	
Indirect costs		
Proratable expenses (% TDC)	10%	1
Field development (% TDC)	10%	
Home Office & construction fee (% TDC)	20%	
Contingency (% TDC)	40%	
Other cost (Start-Up, permits, etc.)	10%	
Materials		
Ethanol ($/kg)	0.999	1
H_2 ($/kg)	1.43	2
Utilities		
Water ($/kJ)	2.24×10^{-7}	1,3
Low pressure steam ($/kJ)	2.00×10^{-6}	
Medium pressure steam ($/kJ)	2.32×10^{-6}	
Fired heat ($/kJ)	4.48×10^{-6}	
Electricity ($/kJ)	1.68×10^{-5}	
Waste management		
Waste treatment ($/kg)	0.0364	4

SI-2 Guerbet coupling catalyst cost estimation

For the estimation of the catalyst cost, we have used the recently developed tool CatCost[5]. This tool allows estimating the cost of a new catalyst to be calculated considering a candidate process and using a reference quantity of catalyst to be produced. In this case, the process was conceived based on the wet impregnation procedure developed by Cuello-Penaloza and coworkers[6]. A schematic of this process is shown in Figure S1. The costs of the catalyst for different ethanol conversions are shown in Table S3. Note that the cost of the catalyst changes with conversion because the size of the lot changes, both as a function of conversion and WHSV.

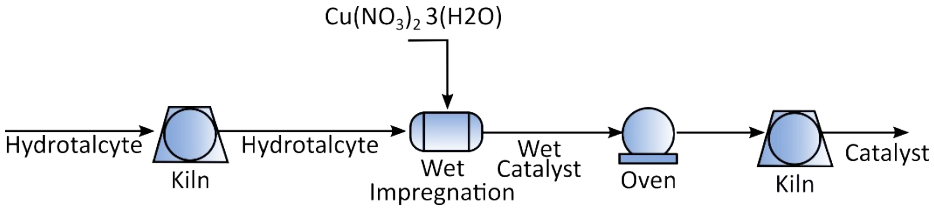

Figure S1. Proposed process for the preparation of the Cu-based catalyst used in this work using wet impregnation

Table S2. Catalyst cost as a function of ethanol conversion

Ethanol conversion (%)	Catalyst cost ($/kg)
12	16.26
15	14.24
20	12.75
40	13.27
66	10.95

SI-3 Catalyst selectivities

The selectivity of the Guerbet coupling reaction as a function of conversion is shown in Table S3. This data is based on the results reported by Cuello-Penaloza and coworkers[7] with minor variations. Some simplification assumptions were applied in this work. These simplifications reduce the set of species that are treated in the process design and are listed below:

- Components with carbon selectivity less than 0.1% are ignored
- All butenes are treated as 1-butene
- All pentenes are treated as 1-pentene
- Linear alcohols with 4 carbons are treated as 1-butanol
- Linear alcohols with 6 carbons are treated as 1-hexanol
- Linear alcohols with 7 carbons are treated as 2-heptanol
- Linear alcohols of 8 carbons are treated as 1-octanol
- Branched alcohols of 8 carbons are treated as 2-ethylhexan-1-ol
- Aromatic alcohols are excluded from calculations for simplicity
- Linear alcohols of 9 carbons are treated as 4-nonanol
- Branched alcohols of 10 carbons are treated as 2-ethyloctan-1-ol
- Branched alcohols of 12 carbons are treated as 2-ethyl-1-decanol
- Aldehydes and ketones are hydrogenated to alcohols
- Acetic acid, 1-methylpropyl ester is treated as butyl acetate
- Acetic acid, 2-ethylbutyl ester is treated as hexyl acetate

- Butanoic acid, 2-ethyl, butyl ester is treated as hexyl butanoate
- Acetic acid, 2-ethylhexyl ester is treated as octyl acetate
- Butyric acid, 2-ethylhexyl ester is treated as octyl butanoate
- 2-ethylbutyl hexanoate is treated as hexyl hexanoate
- Unidentified C14 esters are assumed to be hexyl octanoate
- Unidentified C16 esters are assumed to be octyl octanoate
- We do not consider acetals or hemiacetals in calculations and are treated as their parent alcohols
- Unknown components are distributed proportionally among identified species

Table S3. Carbon selectivity as a function of single-pass ethanol conversion in the Guerbet coupling reaction.

Component	Conversion (%)						
	68.9	**66.5**	**44.2**	**19.1**	**14.5**	**12.3**	**3.1**
Paraffins							
methane	0.10	0.00	0.00	0.00	0.00	0.00	0.00
n-propane	0.10	0.10	0.00	0.00	0.00	0.00	0.00
n-butane	0.00	0.00	0.00	0.00	0.00	0.30	0.00
n-pentane	0.21	0.21	0.00	0.00	0.00	0.00	0.00
Olefins							
ethylene	0.00	0.00	0.00	0.00	0.00	0.00	0.15
1-butene	0.10	0.00	0.22	0.27	0.14	0.15	0.00
1-pentene	0.00	0.42	0.11	0.00	0.00	0.45	0.15
hexenes/dienes/trienes	0.00	0.10	0.00	0.00	0.00	0.00	0.00
Alcohols							
methanol	0.31	0.21	3.11	0.54	0.14	5.89	2.94
isopropanol	2.28	1.14	2.44	1.88	1.66	2.11	13.14
1-butanol	32.82	42.22	53.41	61.51	70.73	69.11	67.70
2-pentanol	4.24	1.46	0.44	0.27	0.14	0.15	0.00
1-hexanol	10.04	13.30	9.11	8.87	7.75	6.19	5.87
2-ethylbutan-1-ol	4.35	4.68	2.67	2.69	2.35	1.81	0.93
2-heptanol	3.42	1.35	1.00	0.67	0.14	0.00	0.00
1-octanol	3.00	4.37	1.67	2.15	1.52	0.91	0.46
2-ethylhexan-1-ol	2.07	2.70	0.78	0.81	0.55	0.30	0.00
4-nonanol	2.59	1.04	0.22	0.40	0.00	0.00	0.00
1-decanol	0.83	1.25	0.33	0.40	0.28	0.00	0.00
2-ethyloctan-1-ol	0.83	0.94	0.33	0.54	0.00	0.00	0.00
4-undecanol	1.04	0.31	0.11	0.00	0.00	0.00	0.00
1-dodecanol	0.62	0.73	0.11	0.13	0.00	0.00	0.00
2-ethyl-1-decanol	0.52	0.83	0.00	0.00	0.00	0.00	0.00
4-tridecanol	0.83	0.42	0.00	0.13	0.00	0.00	0.00
1-tetradecanol	0.10	0.21	0.00	0.00	0.00	0.00	0.00
2-ethyl-1-dodecanol	0.21	0.10	0.00	0.00	0.00	0.00	0.00

1-Pentadecanol	0.52	0.31	0.00	0.00	0.00	0.00	0.00
1-Heptadecanol	0.21	0.00	0.00	0.00	0.00	0.00	0.00
Esters							
methyl acetate	0.21	0.10	0.00	0.54	0.00	0.00	0.00
ethyl acetate	3.42	2.70	10.33	8.19	8.72	8.61	4.64
isopropyl acetate	0.00	0.10	0.00	0.13	0.00	0.00	0.00
ethyl butanoate	5.49	3.43	4.72	3.02	2.42	2.04	0.62
butyl acetate	3.21	2.29	3.78	1.48	1.66	0.91	1.55
butanoic acid, isopropyl ester	0.10	0.10	0.00	0.00	0.00	0.00	0.00
butyl butanoate	4.35	2.60	1.44	0.54	0.28	0.00	0.00
ethyl hexanoate	2.07	1.46	1.22	0.67	0.42	0.30	0.00
hexyl acetate	1.14	0.94	0.78	0.27	0.00	0.00	0.00
butyl hexanonate	3.73	2.70	0.00	0.27	0.00	0.00	0.00
hexyl butanoate	0.52	0.31	1.00	0.13	0.00	0.00	0.00
ethyl octanoate	0.00	0.00	0.00	0.13	0.00	0.00	0.00
octyl acetate	0.31	0.21	0.11	0.94	0.00	0.00	0.00
octyl butanoate	0.31	0.21	0.00	0.27	0.00	0.00	0.00
butyl octanoate	1.76	0.10	0.33	0.13	0.00	0.00	0.00
ethyl decanoate	0.00	1.46	0.00	0.00	0.00	0.00	0.00
decyl acetate	0.10	0.10	0.00	0.54	0.00	0.00	0.00
hexyl hexanoate	0.21	0.21	0.00	0.00	0.00	0.00	0.00
hexyl octanoate	1.04	1.35	0.11	0.40	0.00	0.00	0.00
ethyl dodecanoate	0.10	0.10	0.00	0.00	0.00	0.00	0.00
dodecyl acetate	0.10	0.10	0.00	0.00	0.00	0.00	0.00
Component	**Conversion (%)**						
	68.9	**66.5**	**44.2**	**19.1**	**14.5**	**12.3**	**3.1**
octyl octanoate	0.21	0.31	0.00	0.00	0.00	0.00	0.00
Ethers							
diethyl ether	0.31	0.73	0.11	0.54	0.55	0.00	1.85
3-ethoxy-1-butene	0.00	0.00	0.00	0.54	0.55	0.76	0.00

In tables S4 and S5 we show the selectivity of each alcohol toward ethers and olefins in the etherification reactor. Note that the feed contains multiple reactants and that the numbers in the table represent the fraction of the carbon originally contained in the feedstock that is redirected toward each of the possible products.

Table S4. Carbon selectivity of different alcohols in the etherification reaction when a feedstock similar to the one produced by the Guerbet area with 12% conversion is used. A4: Butanol, A5: 2-pentanol, A6: 1-hexanol, A6-2: 2-ethylbutan-1-ol, A8: 1-octanol, A8-2: 2-ethylhexan-1-ol, E8: di-butyl ether, E10: butyl hexyl ether, E10-2: butyl ethyl butane ether, E12: hexyl ether, E12-4: butyl octyl ether, E14: hexyl octyl ether, O4: butenes, O5: pentenes, O6: hexenes, O8: octenes, UI: unidentified

Reactants	E8	E10	E10_2	E12_4	E12	E14	O5	O4	O6	O8_2	O8	UI
A4	80.68	5.73	0.42	0.04	0.00	0.00	0.00	5.62	0.00	0.00	0.00	7.50
A5	0.00	0.00	0.00	0.00	0.00	0.00	100.00	0.00	0.00	0.00	0.00	0.00
A6	0.00	76.09	0.00	0.00	1.15	8.64	0.00	0.00	10.77	0.00	0.00	3.35
A6-2	0.00	0.00	17.61	0.00	0.00	0.00	0.00	0.00	83.39	0.00	0.00	0.00
A8	0.00	0.00	0.00	5.46	0.00	82.15	0.00	0.00	0.00	0.00	12.39	0.00
A8-2	0.00	0.00	0.00	0.00	0.00	0.00	0.00	0.00	0.00	100.00	100	0.00

Table S5. Carbon selectivity of different alcohols in the etherification reaction when a feedstock similar to the one produced by the Guerbet area with 66% conversion is used. A4: Butanol, A5: 2-pentanol, A6: 1-hexanol, A6-2: 2-ethylbutan-1-ol, A8: 1-octanol, A8-2: 2-ethylhexan-1-ol, E8: di-butyl ether, E10: butyl hexyl ether, E10-2: butyl ethyl butane ether, E12**:** hexyl ether, E12-2: butyl ethyl hexane ether, E12-3: hexyl ethyl butane ether, E12_4: butyl octyl ether, E14: hexyl octyl ether, E14_2: hexyl ethyl hexane ether, E14_3: octyl ethyl butane ether, E16: octyl ether, O4: Butenes, O5: pentenes, O6: hexenes, O7: heptenes, O8: octenes, UI: unidentified

Reactants	E8	E10	E10_2	E12	E12_2	E12_3	E12_4	E14	E14_2	E14_3	E16	O4	O5	O6	O7	O8	UI
A4	62.62	25.79	2.46	0.00	1.42	0.00	5.74	0.00	0.00	0.00	0.00	0.49	0.00	0.00	0.00	0.00	1.48
A5	0.00	0.00	0.00	0.00	0.00	0.00	0.00	0.00	0.00	0.00	0.00	0.00	33.85	0.00	0.00	0.00	66.15
A6	0.00	56.59	0.00	25.20	0.00	2.40	0.00	5.67	1.54	0.00	0.00	0.00	0.00	8.61	0.00	0.00	0.00
A6-2	0.00	0.00	19.99	0.00	0.00	8.88	0.00	0.00	0.00	2.86	0.00	0.00	0.00	14.91	0.00	0.00	53.36
A7	0.00	0.00	0.00	0.00	0.00	0.00	0.00	0.00	0.00	0.00	0.00	0.00	0.00	0.00	90.12	0.00	9.88
A8	0.00	0.00	0.00	0.00	0.00	0.00	44.89	20.19	0.00	2.76	11.46	0.00	0.00	0.00	0.00	20.70	0.00
A8-2	0.00	0.00	0.00	0.00	14.69	0.00	0.00	0.00	7.29	0.00	0.00	0.00	0.00	0.00	0.00	29.32	48.71

Modeling the olefin oligomerization reactions was challenging due to a lack of a kinetic model and/or experimental results for the oligomerization process. To alleviate these limitations, we have relied on an approximation that uses literature data for the oligomerization reactions. In this approach, we assume that each olefin only reacts with itself to form dimers, trimers, and tetramers. Selectivities are estimated considering data available for a HZSM-5 zeolite[8,9]. This approximate treatment is justified because the stream that is oligomerized is small, and represents only ~5% by mass of the total components that are used to produce fuels.

Table S4. Carbon selectivities for the oligomerization catalyst

	Conversion	**dimer**	**trimer**	**tetramer**	**pentamer**	**hexamer**	**References**
1-Butene	95	30.0	22.0	20.0	13.0	15.0	Based on [8]
pentenes	50	90.0	10.0	0.0	0.0	0.0	Based on [9]
hexenes	50	90.0	10.0	0.0	0.0	0.0	Based on [9]
heptenes	50	90.0	10.0	0.0	0.0	0.0	Based on [9]
octenes	50	100.0	0.0	0.0	0.0	0.0	Based on [9]

SI-4 Capital costs

Table S5. Installed costs of the different unit operations used in the Guerbet coupling area for different single-pass ethanol conversions. Costs are $MM

	12%	**15%**	**20%**	**44%**	**66%**
Reactor	27.82	24.95	21.05	12.38	10.08
Compressor 1	1.99	1.99	1.96	1.84	1.78
Compressor 2	1.47	1.45	1.45	1.40	NA
Pumps	0.57	0.53	0.48	0.41	0.39
Flash tank 1	0.49	0.48	0.41	0.25	0.21
Flash tank 2	0.10	0.09	0.09	0.09	NA
Molecular sieves	2.01	2.28	2.35	2.12	1.27
Decanter	NA	NA	NA	NA	0.10
Column 1	7.65	6.60	5.69	7.05	5.48
Column 2	NA	NA	NA	NA	1.20
Column 3	1.63	1.77	2.17	2.12	0.97
Column 4	11.91	7.22	4.02	9.51	4.44
Column 5	33.26	26.77	17.57	10.72	8.62
Column 6	NA	NA	NA	NA	0.53
Column 7	NA	NA	NA	NA	0.73

Table S6. Capital costs of the different unit operations used in the etherification area

	Cost ($MM)
Reactor	8.29
Pumps	0.19
Decanter	0.08
Column 1	5.23
Column 2	6.78
Column 3	5.14
Column 4	2.61
Column 5	1.27

Column 6	4.36
Column 7	1.98
Column 8	0.93
Column 9	1.97
Column 10	2.84
Column 11	6.71
Column 12	1.01
Column 13	11.07

Table S7. Capital costs of the different unit operations used in the oligomerization area

	Cost ($MM)
Reactor	2.53
Pumps	0.46
Molecular sieves	0.11
Column 1	1.94

Table S8. Capital costs of the different unit operations used in the fractionation area

	Cost ($MM)
Column 1	1.01
Column 2	0.70

SI-5 Property calculations

Models from the literature were used to calculate relevant physical properties of the fuel blends produced in this work. Density was calculated for each blend using a linear by volume mixing rule,

$$\rho_{blend} = \sum_{i=1}^{N} f_{V,i}\rho_i \quad , \tag{1}$$

where $f_{V,i}$ is the volume fraction and ρ_i is the density of component *i* in the mixture. Experimental data for the density of each component were used where available. Where data was not available, density was calculated using the GCVOL group contribution method[10].

Liquid kinematic viscosity for each blend (ν) was calculated using the UNIFAC-VISCO method[11].

$$\ln(\nu M) = \sum x_i ln(\nu_i M_i) + \frac{\Delta^* \hat{g}^E}{\hat{R}T} \tag{2}$$

In equation (2), M is the molecular weight of the mixture, x_i, M_i and ν_i are the mole fraction, molecular weight, and kinematic viscosity of component i in the mixture, and $\hat{R}$ and T are the universal gas constant and temperature, respectively. The excess molar free energy of activation for flow ($\Delta^* \hat{g}^E$) is calculated using the UNIFAC-VISCO group contribution method. Details on the theory and required equations to calculate $\Delta^* \hat{g}^E$ are provided elsewhere[11]. The interaction parameters used to calculate the excess Gibbs activation energy are taken from[11,12]. Where experimental data on component viscosity was not available, it was supplemented using the Joback and Reid method[13].

The flash point of the mixtures was modeled using the mixing rule of Liaw et al.[14]

$$\sum \frac{x_i \gamma_i P_{S,i}(T_{FP})}{P_S(T_{FP,i})} = 1 \quad , \tag{3}$$

where x_i is the mole fraction of component i, γ_i is its' activity coefficient, $P_{S,i}(T_{FP})$ is the saturation pressure of component i at the mixture flash point, and $P_S(T_{FP,i})$ is the saturation pressure of component i at its own flash point temperature. To solve this summation, activity coefficients are calculated using the UNIFAC group contribution method[15]. Flash point data for each component were used where available and supplemented with predicted flash points for individual components using the group contribution model of Carroll et al.[16]. Calculation of the component flash point requires knowledge of its' boiling point. Where data were not available, the method of Joback and Reid[13] was again used. Finally, saturation pressures for each component were calculated using the model of Nanoolal et al.[17].

The cloud point of the fuel blend is treated as the thermodynamic equilibrium boundary temperature between the one-phase (liquid) and two-phase (solid/liquid) region for the fuel mixture[18]. Assuming a single component is responsible for the cloud point of the blend and that the heat capacity difference between solid and liquid phases is small relative to the enthalpy of fusion for each component, an expression for the freeze point of component i ($T_{f,i}$) in a mixture can be derived,

$$\frac{1}{T_{f,i}} = \frac{1}{T_{m,i}} - \frac{R \ln\left(x_i^L \gamma_i^L\right)}{\Delta H_{fus,i}(T_{m,i})} \tag{5}$$

where $T_{m,i}$ is the melting point, R is the universal gas constant, x_i^L is the mole fraction, γ_i^L is the activity coefficient, and $\Delta H_{fus,i}(T_{m,i})$ is the enthalpy of fusion for the liquid component in the mixture. Equation (5) is solved to determine the freeze point of each component in the bioblendstock. The cloud point temperature of the bioblendstock is then considered to be the highest predicted freeze point[19,20]. The enthalpy of fusion is estimated for each component using the Joback and Reid method[13]. Experimental data are used for the melting point of each component where available, with the Joback and Reid method again used to supplement for cases where data are not available. Activity coefficients are calculated using the UNIFAC method[15].

Similar to the cloud point, the distillation curve for each blend was calculated as a thermodynamic equilibrium between the liquid and gas phase[21]. The gas phase is treated as ideal, whereas the liquid is again treated non-ideally and characterized by an activity coefficient determined from UNIFAC. Component vapor pressures are calculated using the groups contribution model of Nannoolal et al[17]. A set of *N* differential equations (*N* is the number of components in the blend) are integrated to determine the liquid mole fractions of each component during the distillation using the Rayleigh equation[22]. The determined mole fractions are then used to solve for mixture temperature. Liquid mole fractions are translated into distillate volume assuming ideal mixing behavior.

Finally, the derived cetane number (DCN) was estimated using a simple autoignition model that incorporates group contribution methods to calculate global initiation and chain branching rate constants for each component in the blend[23]. The model was recently developed to provide accurate DCN estimates for oxygenated components and blends with wide ranges of individual cetane numbers, where typical linear by volume mixing rules are no longer sufficient.

The cetane number correlation used in this work is based on data acquired in an ignition quality tester (IQT). The IQT injects fuel into a constant volume chamber and measures the ignition delay in a relatively constant temperature and pressure environment. The measured ignition delay is related to cetane

number through an empirical correlation given in the ASTM D6890 standard and is referred to as the derived cetane number (DCN). In this work, a correlation was used to predict the ignition delay of blends based on a four-step autoignition model.

$$\tau_{mix} = \frac{1}{\sum x_{f,i} k_{\alpha_{p',i}}} \ln\left(1 + \frac{\sum x_{f,i} k_{\alpha_{p',i}}}{\sum x_{f,i} \frac{k_{1_{p',i}}}{x_{c,crit}}}\right) + \tau_{inj}\,.$$

In the equation, $x_{f,i}$ is the mole fraction of component i in the fuel mixture only (i.e., $\sum_{i \neq air} x_{f,i} = 1$). The total initiation rate and net branching coefficient of each component were parameterized assuming they could be written as a sum of contributions from their functional groups.

$$\frac{k_{1_{p',i}}}{x_{c,crit}} = k_{1_0} + \sum k_{1_{f',j}} N_{f,j}$$

$$k_{\alpha_{p',i}} = k_{\alpha_0} + \sum k_{\alpha_{f',j}} N_{f,j}$$

$N_{f,j}$ is the number of functional groups of type j in the compound, and $k_{1_{f',j}}$ and $k_{\alpha_{f',j}}$ are the contributions of function group j to the initiation and chain branching process, respectively. Table 1 specifies all functional groups considered in the model and their respective coefficient values. $k_{\alpha_{p',i}}$ was constrained such that if it made the argument inside the natural log of the ignition delay expression negative after being calculated, it was set to 1E-10 [ms^{-1}] to prevent imaginary numbers from appearing in the results.

The standard ASTM D6890 correlation given by equation was used to transform all ignition delay data in this work.

$$DCN = 4.46 + \frac{186.6}{\tau_{mix}}$$

Table S9. Group contributions for initiation and chain branching determined from optimization procedure

Nomenclature	Description	$k_{1_{f',j}}$ [1/ms]	$k_{\alpha_{f',j}}$ [1/ms]
$N_{f,CH}$	No. CH groups	-2.244E-4	0.2487
$N_{f,CH2}$	No. CH_2 groups	-4.221E-4	0.3099
$N_{f,CH3}$	No. CH_3 groups	-1.453E-4	-0.0404
$N_{f,QC}$	No. quaternary carbons	0.0243	-0.2737
$N_{f,OH}$	No. alcohol groups	0.0131	-1.3357
$N_{f,O=CH}$	No. aldehyde groups	0.0628	-0.0698
$N_{f,-O-}$	No. ether groups	0.0339	0.2854
$N_{f,CH2ring}$	No. CH_2 ring groups	2.917E-4	0.0526
$N_{f,CHring}$	No. CH ring groups	-0.0022	0.2991
$N_{f,C=C}$	No. carbon-carbon double bonds	-0.0012	-0.2285

$N_{f,\,C=O}$	No. ketone groups	-0.003	-0.0928
$N_{f,\,COO}$	No. ester groups	0.0012	-0.8434
$N_{f,AR}$	No. aromatic rings	0.0107	-0.7666
k_{1_0}, k_{α_0}	Constant values	0.0073	-0.0557
τ_{inj}	Constant physical injector delay (0.3206 ms)	-	-

SI-6 Detailed composition of the feed stream for the etherification area

	G-12	**G-66**
Ethanol	0.19	0.00
N-Butanol	91.01	62.88
2-Pentanol	0.16	1.74
1-Hexanol	5.49	13.29
2-ethyl-butanol	1.61	4.67
2-heptanol	0.00	1.16
octanol	0.60	3.27
2-ethyl-hexanol	0.20	2.02
2-heptanol	0.00	0.69
1-octanol	0.00	1.31
2-ethyl-hexanol	0.00	0.17
4-nonanol	0.00	0.36
1-decanol	0.00	0.42
4-tridecanol	0.00	0.19
1-tetradecanol	0.00	0.09
4,10-dimethyl-1 dodecanol	0.00	0.04
1-pentadecanol	0.00	0.12
Ethyl-butyrate	0.37	0.00
N-butyl acetate	0.14	0.00
Isopropyl-butyrate	0.00	0.09
N-butyl-N-butyrate	0.00	1.95
Ethyl-caproate	0.20	1.09
N-hexyl-acetate	0.00	0.70
Butyl-caproate	0.00	1.62
Hexyl-butyrate	0.00	0.19
N-octyl-acetate	0.00	0.12
N-octyl-butyrate	0.00	0.10
Butyl-caprylate	0.00	0.05
Ethyl-caprate	0.00	0.73
Decyl-acetate	0.00	0.05
Hexyl-hexanoate	0.00	0.10

Hexyl-caprylate	0.00	0.58
Ethyl-laurate	0.00	0.04
Dodecyl-acetate	0.00	0.04
1-octanol-octanoate	0.00	0.12
Ethyl-butyl-ether	0.02	0.00

SI-7 Carbon balance in the presence and absence of esters

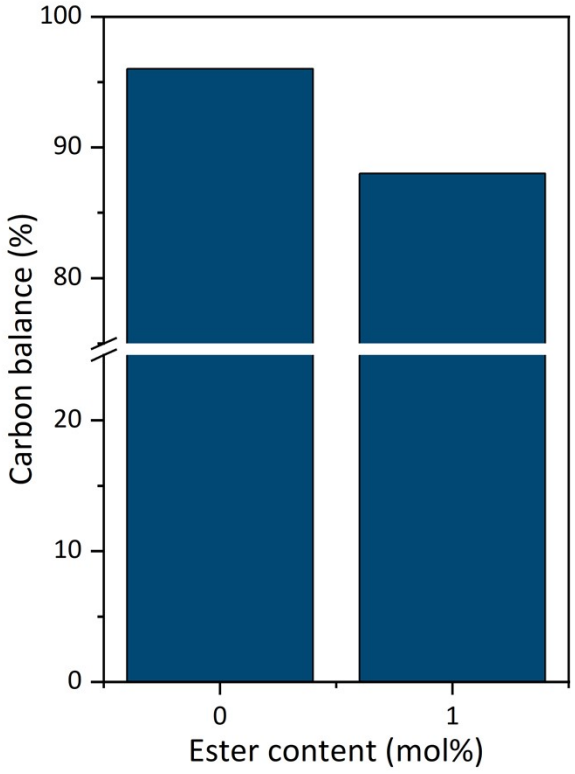

Figure S2. Carbon balance in the presence and absence of esters for the G-12 feedstock

SI-8 Supplemental references

1. Humbird, D. *et al. Process Design and Economics for Biochemical Conversion of Lignocellulosic Biomass to Ethanol: Dilute-Acid Pretreatment and Enzymatic Hydrolysis of Corn Stover*. (2011). doi:10.2172/1013269

2. Tao, L., Markham, J. N., Haq, Z. & Biddy, M. J. Techno-economic analysis for upgrading the biomass-derived ethanol-to-jet blendstocks. *Green Chem.* **19**, 1082–1101 (2017).

3. Aspen Technology, I. Aspen Plus. (2017).

4. Sen, S. M. *et al.* A sulfuric acid management strategy for the production of liquid hydrocarbon fuels via catalytic conversion of biomass-derived levulinic acid. *Energy Environ. Sci.* **5**, 9690–9697 (2012).

5. Guide, U. CatCost. 1–62 (2021).

6. Cuello-Penaloza, P. A. *et al.* Ethanol to distillate-range molecules using Cu/MgxAlOy catalysts with low Cu loadings. *Appl. Catal. B Environ.* **304**, (2022).

7. Cuello-penaloza, P. A. *et al.* Reaction chemistry of ethanol oligomerization to distillate-range molecules using low loading Cu/MgxAlOy catalysts. *Appl. Catal. B Environ.* **318**, 121821 (2022).

8. Bond, J. Q. *et al.* Production of renewable jet fuel range alkanes and commodity chemicals from integrated catalytic processing of biomass. *Energy Environ. Sci.* **7**, 1500–1523 (2014).

9. Maseloane, M. A. Dimerization of naphtha-range Fischer-Tropsch olefins into diesel-range products over zeolite H-ZSM-5 and amorphous silica-alumina. (University of Cape Town, 2011).

10. Ihmels, E. C. & Gmehling, J. Extension and revision of the group contribution method GCVOL for the prediction of pure compound liquid densities. *Ind. Eng. Chem. Res.* **42**, 408–412 (2003).

11. Gaston-Bonhomme, Y., Petrino, P. & Chevalier, J. L. UNIFAC-VISCO group contribution method for predicting kinematic viscosity: extension and temperature dependence. *Chem. Eng. Sci.* **49**, 1799–1806 (1994).

12. Bandrés, I., Lahuerta, C., Villares, A., Martín, S. & Lafuente, C. Kinematic viscosities for ether + alkane mixtures: Experimental results and UNIFAC-VISCO parameters. *Int. J. Thermophys.* **29**, 457–467 (2008).

13. Joback, K. G. & Reid, R. C. Estimation of Pure-Component Properties from Group-Contributions. *Chem. Eng. Commun.* **57**, 233–243 (1987).

14. Liaw, H. J. & Chiu, Y. Y. A general model for predicting the flash point of miscible mixtures. *J. Hazard. Mater.* **137**, 38–46 (2006).

15. Fredenslund, A., Gmehling, J. & Rasmussen, P. *Standard test method for distillation of petroleum products at reduced pressure*. (Elsevier, 1986). doi:10.1520/mnl10861m

16. Carroll, F. A., Lin, C. Y. & Quina, F. H. Simple method to evaluate and to predict flash points of organic compounds. *Ind. Eng. Chem. Res.* **50**, 4796–4800 (2011).

17. Nannoolal, Y., Rarey, J. & Ramjugernath, D. Estimation of pure component properties part 3. Estimation of the vapor pressure of non-electrolyte organic compounds via group contribution and group interactions. *Fluid Phase Equilib.* **269**, 117–133 (2008).

18. Mirante, F. I. C. & Coutinho, J. A. P. Cloud point prediction of fuels and fuel blends. *Fluid Phase Equilib.* **180**, 247–255 (2001).

19. Imahara, H., Minami, E. & Saka, S. Thermodynamic study on cloud point of biodiesel with its fatty acid composition. *Fuel* **85**, 1666–1670 (2006).

20. Seniorita, L., Minami, E. & Kawamoto, H. Development and Evaluation of Thermodynamic Models for Predicting Cold Flow Properties of Biodiesel. *J. Adv. Res. Fluid Mech. Therm. Sci.* **76**, 117–125 (2020).

21. Ferris, A. M. & Rothamer, D. A. Methodology for the experimental measurement of vapor-liquid equilibrium distillation curves using a modified ASTM D86 setup. *Fuel* **182**, 467–479 (2016).

22. Stichlmair, J. G. & Klein, H. *Distillation: principles and practice*. (John Wiley & Sons, 2021).

23. Dustin Witkowski & Rothamer, D. A. Simple autoignition model for the derived cetane number of oxygenated compounds and fuel blends. in *Spring Technical Meeting of The Central States Section of the Combustion Institute,* (2022).